Journal of Applied Sciences

ISSN 1812-5654

science alert

ANSInet
an open access publisher
http://ansinet.com

Journal of Applied Sciences 9 (7): 1331-1337, 2009
ISSN 1812-5654

Finite Element Analysis of Thickness Effect on the Residual Stress in Butt-Welded 2.25Cr1Mo Steel Plates

F. Vakili-Tahami and A.H.D. Sorkhabi
Department of Mechanical Engineering, University of Tabriz, Tabriz 51666-16471, Iran

Abstract: In this study, a numerical method is presented to study the thickness effect on the residual stress states in butt-welds in 2.25Cr1Mo plates. Using finite element based software ANSYS, coupled thermal-mechanical three dimensional (3D) finite element models have been developed. The finite element models are employed to evaluate the transient temperature and the residual stress fields during welding. Also, in this study the variations of the physical and mechanical properties of the material with temperature have been taken into account. Results show that by increasing plate thickness, the residual stresses increase and the residual stress affected zone (distance with significant amount of residual stress) becomes larger. It has been shown that the longitudinal residual stress in weld axis, change from compressive to tensile stress by increasing plate thickness.

Key words: Finite element, welding residual stress, thickness, 2.25Cr1Mo steel

INTRODUCTION

2.25Cr1Mo steels are widely used in both nuclear as well as conventional power plants. Heavy-wall pressure vessels and pipes are often constructed from this type of Cr-Mo steel because of its excellent high-temperature strength. Therefore welded joints of Cr-Mo ferrite steels play very important role in the power industry. Hence mechanical behaviors' weld ability and Post Welding Heat Treatment (PWHT) of Cr-Mo steels have been extensively studied in recent decades. The advantages of welding, as a joining process, include high joint efficiency, simple set up, flexibility and low fabrication costs. Even though it has many positive properties, fusion welding can alter the properties of the material and may causes deflection, shrinkage and residual stresses in the joint (Richards *et al*., 2008).

Thermal stresses are generated during welding due to the non- uniform temperature distribution around the joint. As the temperature of the base metal increases, the yield strength decrease and the thermal stresses increase. It is well known that resulting residual stresses have a strong influence on weld deformation, fatigue, fracture, creep and buckling. Thus, it is important to analyze the residual stresses due to welding. To determine the residual stresses around a welded joint both non-destructive and destructive test methods can be used, these methods include X-ray diffraction, ultrasonic analysis, hole drilling and sectioning. These methods are expensive or destructive, therefore numerical methods are becoming a major tool to study the mechanical behaviour of the weldments. These methods, which provide detailed analysis of the residual stresses due to welding, have developed considerably during the last three decades due to the improvements in computers and in the numerical techniques. These developments are the work of Hibbitt and Marcal who developed numerical thermal- mechanical models using the finite element method (Hibbitt and Marcal, 1973). Lee and Chang (2007) have also developed a 3D FE model to calculate the residual stresses in welds. Murugan *et al*. (2001) have proposed a numerical model for multi-pass welding and a material database for toughness of butt-welded assemblies used in heavy structures. Deng and Murakawa (2006) have produced the simulation results which show that both volumetric and yield strength changes have significant effects on welding residual stress in 2.25Cr1Mo steel pipes. The effect of residual stresses on the fatigue strength in a weld toe for a multi-pass fillet weld joint has been investigated by Messler (2004).

In this study, the butt-welding of two 2.25Cr1Mo plates has been modeled using FEM based software. To study the thickness effect on the residual stresses in butt-welds, three cases with different plate thickness have been analyzed. A 3D finite element model has been developed and the movement of the electrode has been simulated using the death and birth of elements. For this purpose a coupled thermo-mechanical solution method

Corresponding Author: Amir H.D. Sorkhabi, Department of Mechanical Engineering, University of Tabriz, Tabriz 51666-16471, Iran

has been used. The elasto-plastic temperature dependent material behaviour has also been taken into account. In this way, the along-weld-joint and through thickness residual stresses and also effect of thickness on the residual stress have been obtained.

WELD METALLURGY

Fusion welding involves the localized injection of intense heat and its dissipation by conduction into the parent material. The weld microstructure at each location is therefore closely related to the thermal history (Parmar, 1999). The different zones and their characteristics have been described for a single pass weld by Mannan and Laha (1996) and are shown in Fig. 1. Regardless of the primary solidification, the fusion zone in low alloy steel transforms to austenite at a temperature not far from its solidification point and then undergoes a solid state transformation to a structure that will depend on both the harden ability of the alloy and the cooling rate (Mannan and Laha, 1996).

Adjacent to the fusion zone is a Heat Affected Zone (HAZ); a region that is not heated sufficiently to cause melting, but nevertheless has been altered by the welding thermal cycle. As shown in Fig. 1, the HAZ can be subdivided according to the extent to which grain growth and austenitisation occur; into a coarse grained zone (CGHAZ), a fine grained zone (FGHAZ), an intercritical zone (ICHAZ) and over tempered base metal. Fusion welding of thick walled components necessarily involves many weld passes to fill up the joint. Weld beads covered by other passes then experience multiple heat pulses and a further subdivision of metallurgical zones (Kou, 2003).

RESIDUAL STRESS

When steel structures are welded, a localized fusion zone is generated in the weld joint because of the high heat input from the arc and then nonuniform temperature distribution is induced due to the heat conduction. Therefore, nonuniform heat deformation and thermal stresses are included in the as-welded parts. As a result, plastic deformation is retained within the weldment and nonlinear plastic deformation and residual stresses exist after cooling of the welded joint.

Different parameters determine the amount of the residual stresses and its distribution pattern in welded joints. The major parameters are (Leggatt, 2008):

- The geometry of the parts being jointed
- The material properties of the weld and parent materials, including composition, microstructure, thermal properties and mechanical properties
- Residual stresses which exist in the parts before welding, resulting from the processes used to manufacture the components and fabrication operations prior to welding
- Residual stresses generated or relaxed by manufacturing operations after welding or by thermal or mechanical loading during service life

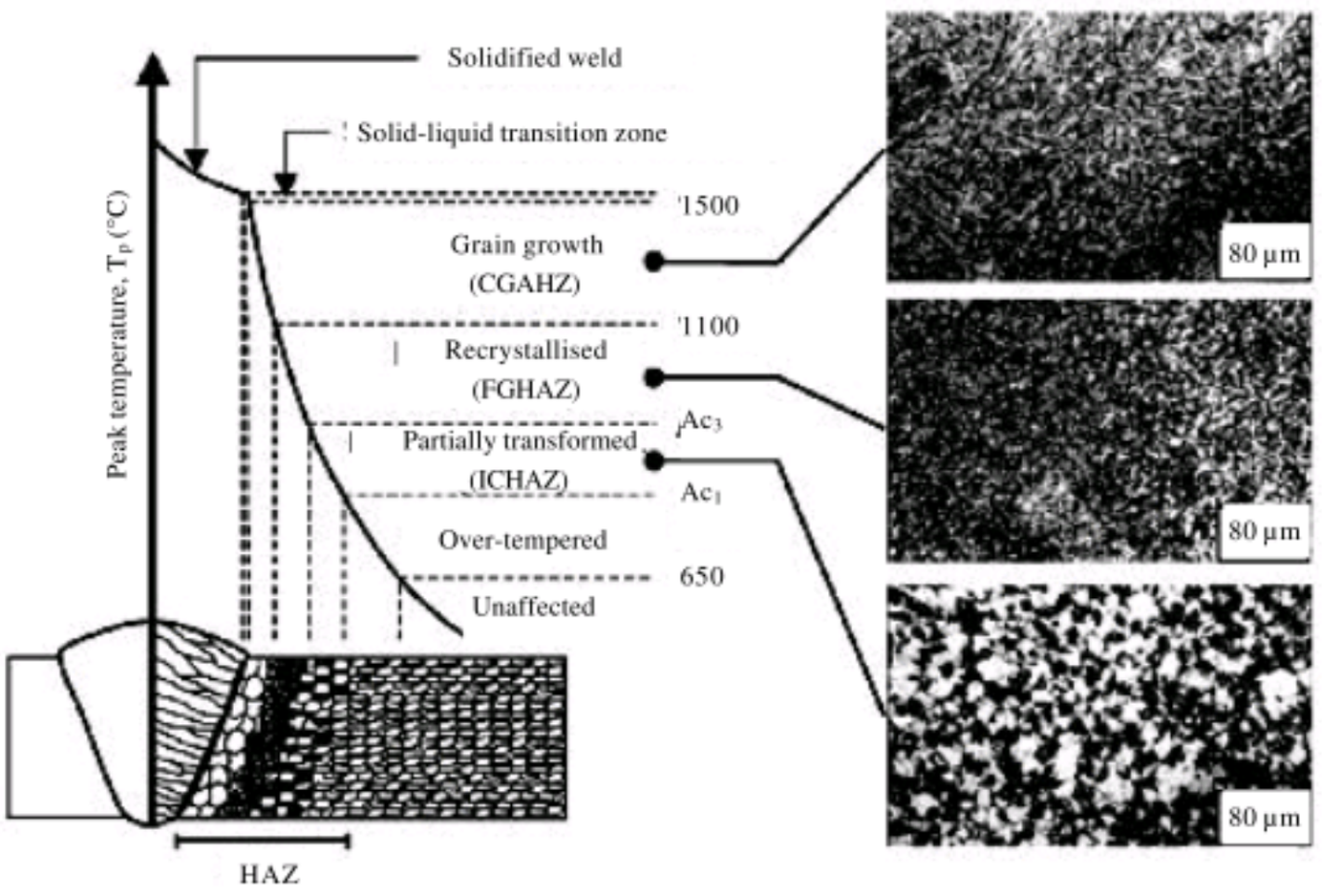

Fig. 1: Metallurgical zones in single pass weld, categorized according to the maximum local temperature and micrographs, which, corresponds to the weld in 2.25Cr1Mo steel (Francis *et al*., 2007)

FINITE ELEMENT MODELING

The analytical algorithm used in this study to calculate the residual stresses due to the welding is shown in Fig. 2.

The commercial finite element code ANSYS has been used to carry out the thermal and mechanical analysis. A sequentially coupled analysis of thermal and mechanical analysis has been performed. In coupled thermo-mechanical analysis, there are 4 degrees of freedom which one is the temperature. This method will increase the accuracy of the model and also takes into account the mutual effects of thermal strains and temperature. Also, a bi-linear elasto-plastic model has been used to carry out the stress analysis. The geometry of the model considered in this study is shown in Fig. 3.

Two semi-infinite plates of the joint are 4 mm thick and 72 mm width (along the welding direction). In two other case studies, thicknesses of the plates are 6 and 8 mm. The weld-groove angle is 60° and due to the symmetry, only half of the weld and plates have been modeled. The chemical composition of 2.25 Cr1Mo low-alloy-ferritic steel plates used in this study is shown in Table 1 (Kelly and Joseph, 1993).

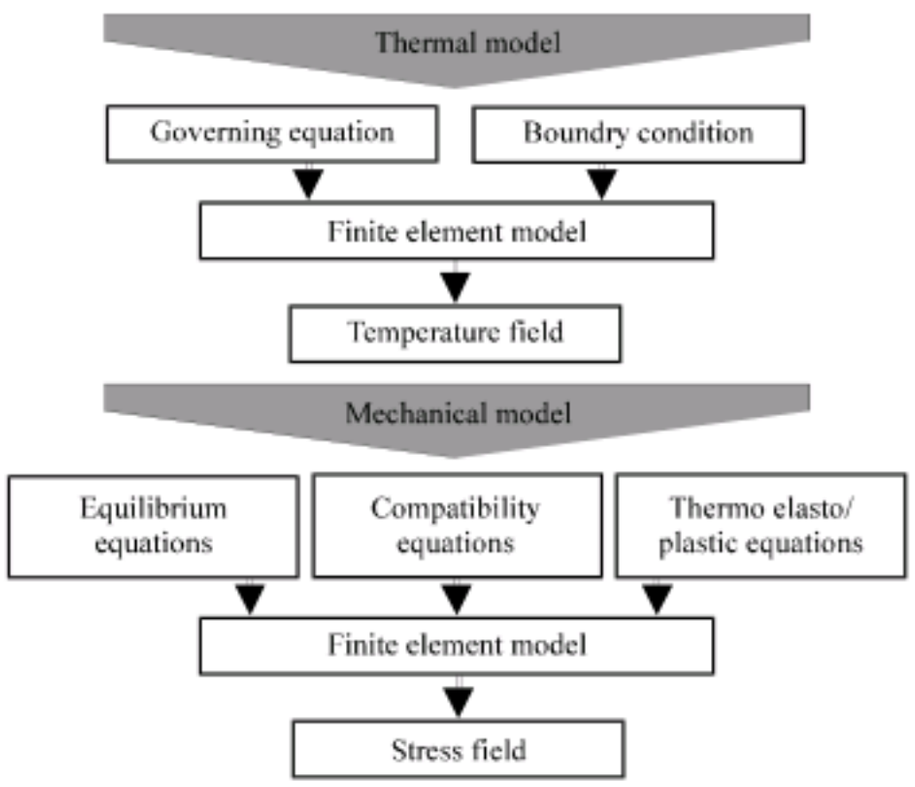

Fig. 2: Flowchart of residual stress analysis

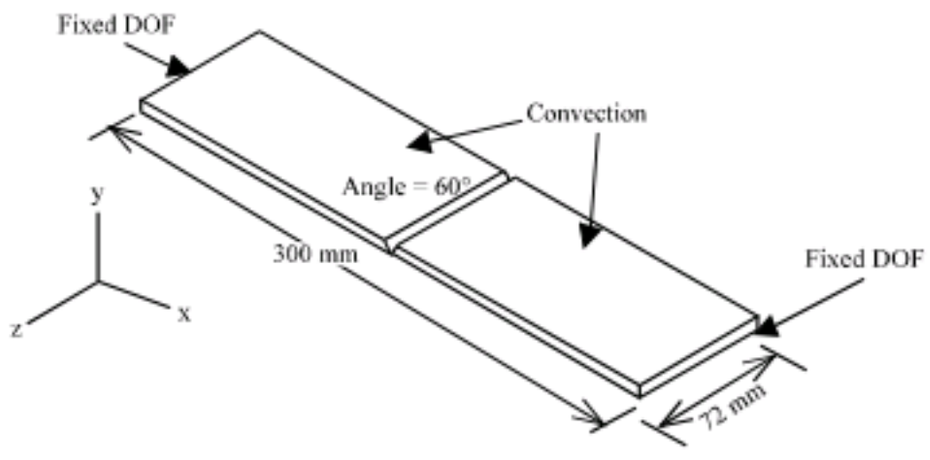

Fig. 3: Joint configuration and FE boundary conditions for two semi-infinite 2.25Cr1Mo low-alloy-ferritic steel plates

Welding residual stresses are a consequence of interactions time, temperature, deformation and microstructure. Physical and mechanical properties that influence the development of welding residual stresses include thermal conductivity, heat capacity, thermal expansion coefficient, elastic modulus and Poisson's ratio, yield strength, work hardening coefficient. Yield magnitude residual stresses may occur if the thermal strain during cooling after welding is greater than the yield strain, that is if:

$$\alpha (T_s - T_0) \geq \sigma_Y / E \quad (1)$$

where, α is the coefficient of thermal expansion, T_s is the softening temperature, defined here as the temperature at which the yield strength drops to 10% of its value at ambient temperature, T_o is the ambient or uniform pre-heat temperature, E is the Young's modulus, σ_Y is the yield strength at ambient or pre-heat temperature (Leggatt, 2008).

The temperature- dependent thermo-physical and mechanical properties of the 2.25Cr1Mo steels are shown in Fig. 4, respectively (Deng and Murakawa, 2008). The temperature of the melted filler material is set to be 1510°C. Since the plate can dissipate heat through convection, the heat transfer coefficient on the plate surface is assumed to be 12 J/m^2/s/K.

Thermal model: During welding the governing partial differential equation for 3D transient heat conduction, with heat generation rate Q, heat flux rate and considering density ρ, thermal conductivity k and specific heat c as functions of temperature only, is given by the thermal equilibrium equation:

$$\rho c \frac{\partial T}{\partial t}(x,y,z,t) = -\nabla . q(x,y,z,t) + Q(x,y,z,t) \quad (2)$$

In all of the welding processes, a heat source provides the required energy and causes localized high temperature spot. To simulate arc heating effects during welding, the equivalent heat input can be assumed as the combination of both surface and body heat flux components (Bang *et al*., 2002). The total heat input can be given as follows:

Table 1: Chemical composition of the 2.25 Cr1Mo low alloy ferritic steel (%)

C	Si	Mn	P	S	Cr	Mo	Cu
0.06-0.15	0.5	0.4-0.7	0.035	0.03	2-2.5	0.9-1.1	0.3

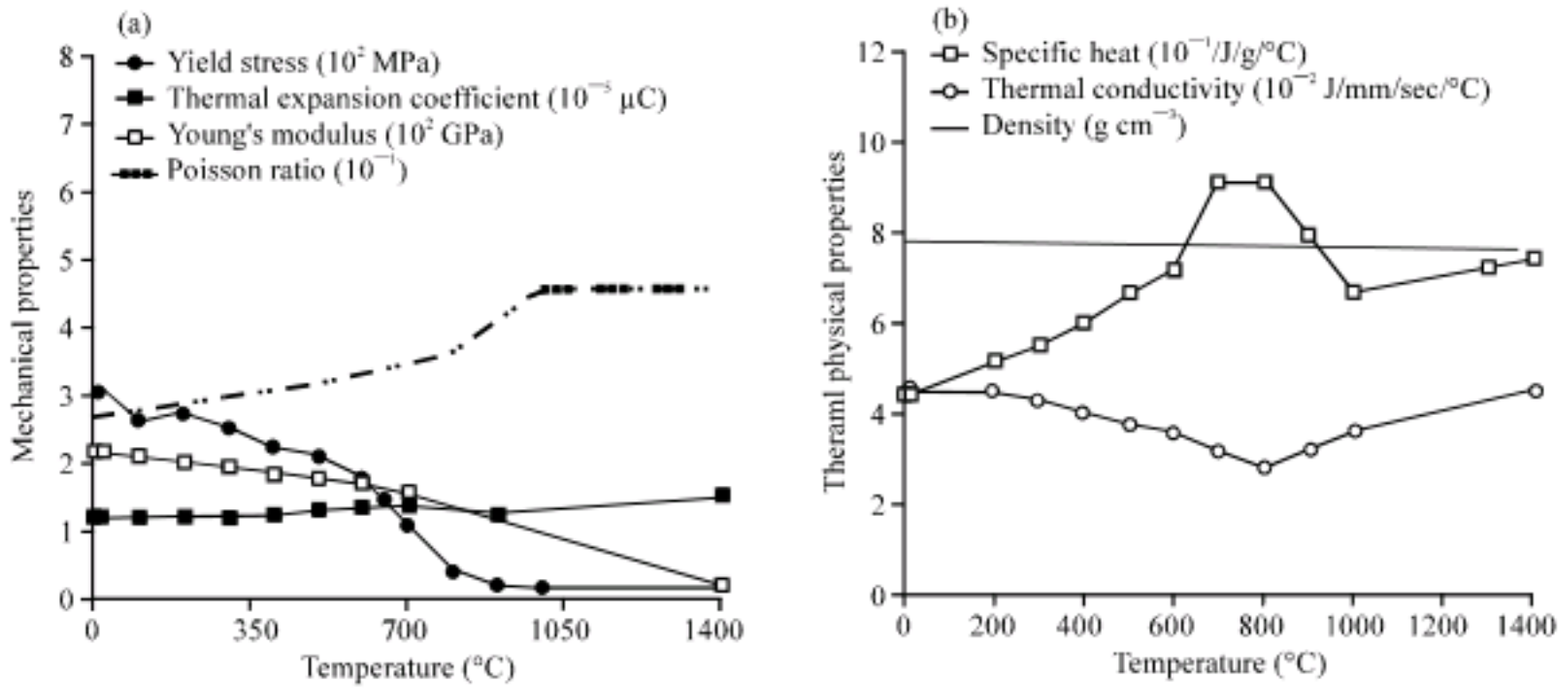

Fig. 4: (a) Temperature-dependent thermal mechanical properties and (b) Temperature-dependent thermal physical properties (Deng and Murakawa, 2008)

$$Q = Q_s + Q_b = \eta EI \quad (3)$$

where, Q_s and Q_b are the heat input due to surface flux and body flux, respectively, η is the arc efficiency, E is voltage and I is current. The ratio of Q_b/Q_s can be adjusted to achieve an accurate representation of the fusion zone. In this study, the total heat input was assumed to be 20% of surface flux and 80% of body flux which are based on the experimental data and the calculated size of the fusion zone. The arc efficiencies used in the analysis are 0.75 for SMAW and 0.40 for GTAW. The surface flux q_s and body flux q_b are generally represented in the form of a Gaussian distribution as follows:

$$q_s = \frac{3Q_s}{\pi ac}\exp\left(-\frac{3x^2}{a^2}-\frac{3z^2}{c^2}\right) \quad (4)$$

$$q_b = \frac{6\sqrt{3}Q_b}{abc\pi\sqrt{\pi}}\exp\left(-\frac{3x^2}{a^2}-\frac{3y^2}{b^2}-\frac{3z^2}{c^2}\right) \quad (5)$$

where, a, b and c are the semicharacteristic arc dimensions in x, y and z direction. This heat source model has often been used to approximate simple welding processes carried out in the flat position, i.e., welding horizontally in a straight line on a horizontal flat plate with the electrode perpendicular to the plate. A characteristic of a low-hydrogen electrode is often a shallow penetration, which suggests a heat distribution flatter and more evenly distributed than Gaussian. Sabapathy *et al*. (2000) modified the Gaussian heat source model by changing the exponential terms have used this model to simulate in-service welding (Sabapathy *et al.,* 2000). In this study, the heat fluxes of Eq. 4 and 5 were modified by assuming the uniform distribution of heat fluxes in width and thickness direction in order to simulate the shallow penetration of heat. The surface and body fluxes can be given as follows:

$$q_s = \frac{\sqrt{3}Q_s}{ac\sqrt{\pi}}\exp\left(-\frac{3z^2}{c^2}\right) \quad (6)$$

$$q_b = \frac{\sqrt{3}Q_b}{Ac\sqrt{\pi}}\exp\left(-\frac{3z^2}{c^2}\right) \quad (7)$$

where, A is the cross-sectional area of the fusion zone. The values of a and c were chosen as the half width of the fusion zone. The fixed z-coordinate is related to the moving coordinate as follows:

$$z = \nu(\tau - t) \quad (8)$$

where, ν is the welding speed and τ is a lag factor to define the position of the heat source at time t = 0 (Bang *et al*., 2002).

Mechanical model: Two basic sets of equations relating to the mechanical model, the equilibrium equations and the constitutive equations are considered as follows:

- Equations of equilibrium

$$\sigma_{ij} + \rho b_i = 0 \quad (9)$$

$$\sigma_{ij} = \sigma_{ji} \quad (10)$$

where, σ_{ij} is the stress tensor and b_i is the body force.

- Constitutive equations for a thermal elastoplastic material

The thermal elastoplastic material model, based on the Von Mises yield criterion and the isotropic strain hardening rule, is considered. Stress-strain relations is written as:

$$[d\sigma] = [D^{ep}][d\varepsilon] - [C^{th}]dT \quad (11)$$

$$[D^{ep}] = [D^{e}] + [D^{p}] \quad (12)$$

where, $[D^e]$ is the elastic stiffness matrix, $[D^p]$ is the plastic stiffness matrix, $[C^{th}]$ is the thermal stiffness matrix, $d\sigma$ is the stress increment, $d\varepsilon$ is the strain increment and dT is the temperature increment (Chang and Teng, 2004).

Analysis model: The high temperature around the welding pool and the existing heat dissipation through the plate and from the surface cause a severe temperature gradient, which change the microstructure of the metal next to the welded joint. Although, the Heat Affected Zone (HAZ) itself is composed of different layers, but in this model, it has been regarded as one layer and its physical properties are shown in Fig. 4. with temperature.

To model the movement of the welding electrode along the z-axis (Fig. 3), the weld has been divided into 3 parts and each part has 24 mm lengths (Fig. 5). With the speed of 3 mm sec^{-1} for the movement of the welding electrode, each part will take 8 sec to finish which will be called a step. These values have been adapted based on the Rosenthal's model and he has proved that in this way, the temperature in each part can be assumed to be constant (Messler, 2004). In each step, these parts have been added to the weldment (FE mesh) using Birth and Death technique. The heat input has been applied to each part for 8 sec. After one step, the elements of the second part have been introduced to the FE mesh (birth of elements) and the heat source has been removed from the earlier part and has been applied to the second part. By repeating this pattern, the third part has been introduced until the welding has been completed.

RESULTS AND DISCUSSION

The thermal analysis has shown that after cooling, the plate reaches the steady state temperature distribution. Therefore, the residual stresses at this stage have been presented here. Also, to capture the variation of residual stress distribution (longitudinal stress) along the plate as well as the plate thickness, three paths have been defined along the x-axis and are shown in Fig. 5.

Comparisons of the results show the effect of the plate thickness on the welding residual stresses.

It can be seen that along this path, by increasing the plate thickness, the longitudinal residual stress in the weld axis increases significantly from 165 MPa for 4 mm plate to 233 MPa for 8 mm plate (Fig. 6). Also the absolute amount of the compressive residual stress in the parent material increases from -23.5 MPa for 4 mm plate to -54.5 MPa for 8 mm plate. Figure 6 also shows that the distance in which the longitudinal residual stress changes from maximum tensile to minimum compressive level, increases from $0<x<11$ mm for 4 mm plate to $0<x<13$ mm for 8 mm plate. It can be shown from Fig. 6, that the residual stresses reach almost zero level in $x \approx 60$ mm, however this distance is slightly larger for plate with larger thickness.

Figure 7 shows that the plate thickness has a significant effect on the weld-axis residual stresses. For plate with 4 mm thickness, the accumulation of heat due to the welding of the earlier part, have led to a significant reduction in stress level at the weld-axis: -5 MPa for 4 mm plate comparing with 310 MPa for the plate with 6 mm thickness and 660 MPa for the plate with

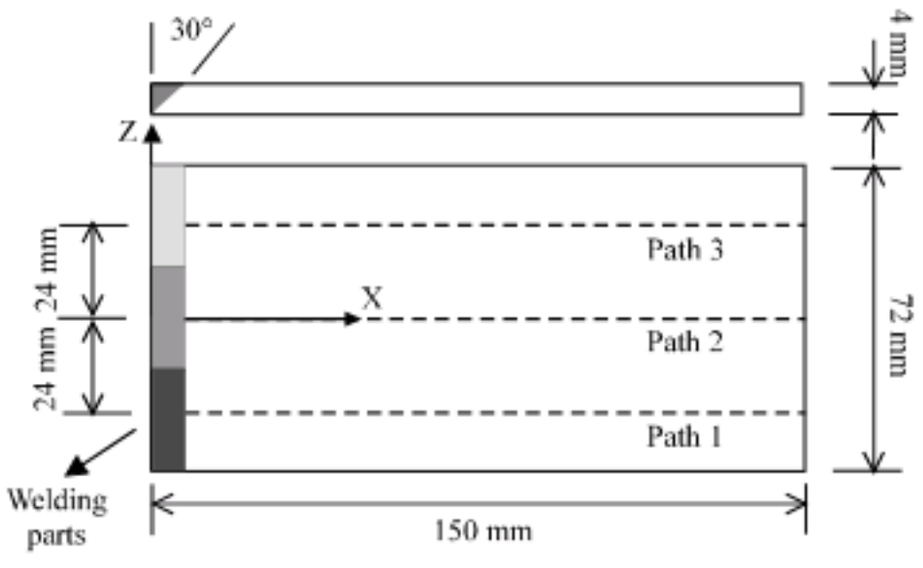

Fig. 5: Three paths defined in welded plates to present the results

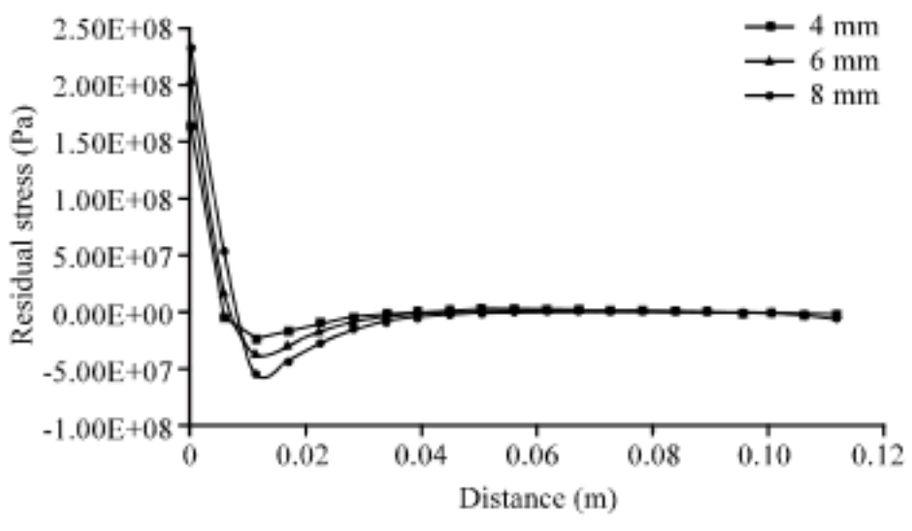

Fig. 6: Distribution of the longitudinal residual stresses (σ_z) along path 1 on the plate surface

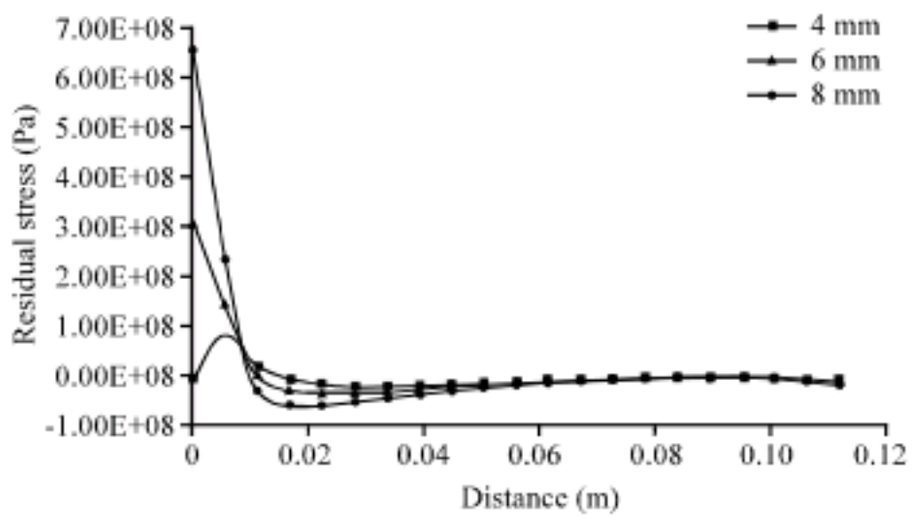

Fig. 7: Distribution of the longitudinal residual stresses (σ_z) along path 2 on the plate surface

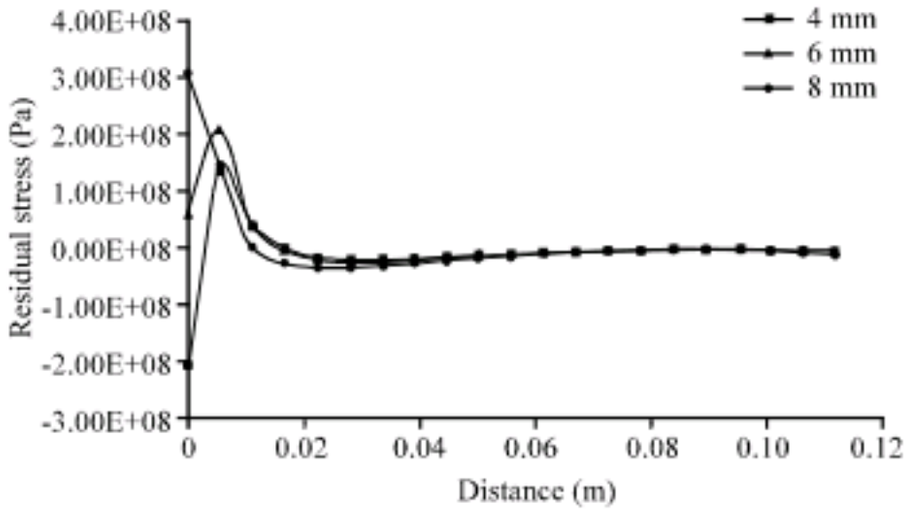

Fig. 8: Distribution of the longitudinal residual stresses (σ_z) along path 3 on the plate surface

8 mm thickness. This effect is becoming more dominated along path 3 at Fig. 8. Figure 8 shows that the plate thickness has a significant effect on the weld-axis residual stresses. For plate with 4 mm thickness, the accumulation of heat due to the welding of the earlier part, have led to a significant reduction in stress level at the weld-axis: -200 MPa for 4 mm plate comparing with 60 MPa for the plate with 6 mm thickness and 300 MPa for the plate with 8 mm thickness. As it can be seen in Fig. 8. the weld-axis longitudinal residual stress level for both 4 and 6 mm plates have been decreased. Also it shows that unlike plate with 8 mm thickness, the location of the maximum tensile stress for 4 and 6 mm plates has been shifted to the HAZ.

CONCLUSION

In this study, an FE based 3D model has been used to calculated the residual stresses for a butt-welded joint. Also the effect of plate thickness on the residual stresses has been studied.

The results show that:

- Using 3D model produce more accurate results. The different patterns for residual stress distribution along three paths, confirms that the use of 2D models will lead to erroneous results
- Using element Birth and Death technique is a powerful tool to accommodate the weld arc movement in a 3D FE model to carry out thermo-mechanical analysis
- Due to the sever temperature gradient, the variation of physical and mechanical parameters with temperature should be taken into account
- By increasing plate thickness (from 4 to 8 mm), in the same condition, the residual stresses increase by almost 70%
- By increasing plate thickness, the residual stress affected zone (distance with significant amount of residual stress) becomes larger
- The longitudinal residual stress in weld axis, change from compressive stress for 4 mm plate to tensile stress for 8 mm plate, along path 2 and 3 (Fig. 7, 8). This shows that the pattern of residual stress distribution changes along the electrode movement direction

REFERENCES

Bang, B., Y. Son, K. Oh, Y. Kim and W. Kim, 2002. Numerical simulation of sleeve repair welding of in-service gas pipelines. Weld. J., 81: 273.S-282.S.

Chang, P.H. and T.L. Teng, 2004. Numerical and experimental investigations on the residual stresses of the butt-welded joints. Comput. Mater. Sci., 29: 511-522.

Deng, D. and H. Murakawa, 2006. Numerical simulation of temperature field and residual stress in multi-pass welds in stainless steel pipe and comparison with experimental measurements. Comput. Mater. Sci., 37: 269-277.

Deng, D. and H. Murakawa, 2008. Finite element analysis of temperature field, microstructure and residual stress in multi-pass butt-welded 2.25Cr-1Mo steel pipes. Comput. Mater. Sci., 43: 681-695.

Francis, J.A., H.K.D.H. Bhadeshia and P.J. Withers, 2007. Welding residual stresses in ferritic power plant steels. Mater. Sci. Technol., 23: 1009-1020.

Hibbitt, H.D. and P.V. Marcal, 1973. A numerical thermo-mechanical model of the welding and subsequent loading of a fabricated structure. Comput. Struct., 3: 1145-1174.

Kelly, F. and R.D. Joseph, 1993. ASM Handbook: Vol. 6. Welding, Brazing and Soldering. 10th Edn., ASM International, Materials Park, OH., ISBN: 0-87170-382-3, pp: 1299.

Kou, S., 2003. Welding Metallurgy. 1st Edn., John Wiley and Sons, Hobokon, New Jersey, ISBN: 0-471-43491-4, pp: 480.

Lee, Ch.H. and K.H. Chang, 2007. Three-dimensional finite element simulation of residual stresses in circumferential welds of steel pipe including pipe diameter effects. Mater. Sci. Eng. A, 487: 210-218.

Leggatt, R.H., 2008. Residual stresses in welded structures. Int. J. Pressure Vessels Piping., 85: 144-151.

Mannan, S.L. and K. Laha, 1996. Creep behaviour of Cr–Mo steel weldments. Trans. Indian. Inst. Metals, 49: 303-320.

Messler, R.W., 2004. Principles of welding. Wiley-Vch.

Murugan, S., S.K. Rai, P.V. Kumar, Y. Kim, W. Jayakumar, B. Raj and M.C.S. Bose, 2001. Temperature distribution and residual stresses due to multipass welding in type 304 stainless steel and low carbon steel weld pads. Int. J. Pressure Vessels Piping, 78: 307-317.

Parmar, R.S., 1999. Welding Engineering and Technology. 1st Edn., Khanna Publishers, Delhi, ISBN: 81-7409-028-2.

Richards, D.G., P.B. Prangnell, S.W. Williams and P.J. Withers, 2008. Global mechanical tensioning for the management of residual stresses in welds. Mater. Sci. Eng. A, 489: 351-362.

Sabapathy, P.N., M.A. Wahaba and M.J. Painter, 2000. The prediction of burn-through during in-service welding of gas pipelines. Int. J. Pressure Vessels Piping, 77: 669-677.